NeuroImage: Clinical 23 (2019) 101916

Contents lists available at ScienceDirect

NeuroImage: Clinical

journal homepage: www.elsevier.com/locate/ynicl

White and gray matter brain development in children and young adults with phenylketonuria

Zoë Hawks[a,*,1], Anna M. Hood[a,1,2], Dov B. Lerman-Sinkoff[a,b], Joshua S. Shimony[c], Jerrel Rutlin[c], Daniel Lagoni[a], Dorothy K. Grange[d], Desirée A. White[a,d]

[a] Department of Psychological & Brain Sciences, Campus Box 1125, Washington University, St. Louis, MO, United States
[b] Department of Biomedical Engineering, Washington University, St. Louis, MO, United States
[c] Mallinckrodt Institute of Radiology, Washington University School of Medicine, St. Louis, MO, United States
[d] Department of Pediatrics, Washington University School of Medicine, St. Louis, MO, United States

ARTICLE INFO

Keywords:
Phenylketonuria
Brain
White matter
Gray matter
Developmental trajectories
Executive abilities

ABSTRACT

Phenylketonuria (PKU) is a recessive disorder characterized by disruption in the metabolism of the amino acid phenylalanine (Phe). Prior research indicates that individuals with PKU have substantial white matter (WM) compromise. Much less is known about gray matter (GM) in PKU, but a small body of research suggests volumetric differences compared to controls. To date, developmental trajectories of GM structure in individuals with PKU have not been examined, nor have trajectories of WM and GM been examined within a single study. To address this gap in the literature, we compared longitudinal brain development over a three-year period in individuals with PKU (n = 35; 18 male) and typically-developing controls (n = 71; 35 male) aged 7–21 years. Using diffusion tensor imaging (DTI) and structural magnetic resonance imaging (MRI), we observed whole-brain and regional WM differences between individuals with PKU and controls, which were often exacerbated with increasing age. In marked contrast with trajectories of WM development, trajectories of GM development did not differ between individuals with PKU and controls, indicating that neuropathology in PKU is more prominent in WM than GM. Within individuals with PKU, mediation analyses revealed that whole-brain mean diffusivity (MD) and regional MD in the corpus callosum and centrum semiovale mediated the relationship between dietary treatment compliance (i.e., Phe control) and executive abilities, suggesting a plausible neurobiological mechanism by which Phe control may influence cognitive outcomes. Our findings clarify the specificity, timing, and cognitive consequences of whole-brain and regional WM pathology, with implications for treatment and research in PKU.

1. Introduction

Phenylketonuria (PKU; OMIM212600) is an autosomal recessive disorder characterized by an error in the metabolism of the amino acid phenylalanine (Phe) (Dyer, 1999). Deficiency in or absence of the phenylalanine hydroxylase enzyme (PAH; EC # 1.14.16.1) results in decreased tyrosine (a precursor to catecholaminergic neurotransmitters) and accumulation of Phe at substantially higher than normal levels in blood and tissue (Scriver, 2007). PKU occurs in all ethnic groups (Hardelid et al., 2008), with an estimated worldwide prevalence of 1 in 10,000 live births (Waters et al., 2018). When untreated, the neurotoxic accumulation of Phe results in severe intellectual disability (Anderson et al., 2007). However, the most serious cognitive sequelae are now generally avoided through early detection and dietary treatment to limit Phe intake (Waisbren et al., 2007). Notwithstanding, individuals with early-and continuously-treated PKU experience neuropsychological impairment (Araujo et al., 2009; Banerjee et al., 2011; Christ et al., 2006; Hawks et al., 2018; Janos et al., 2012), particularly related to executive abilities (Christ et al., 2010; Jahja et al., 2017).

The neurobiological underpinnings of executive dysfunction in PKU are incompletely understood, although white matter (WM) compromise appears to play an important role (Anderson et al., 2007; Hood et al., 2016, 2015). Gross WM abnormalities, assessed through visual inspection of structural magnetic resonance images (MRI), have long been

* Corresponding author at: Department of Psychological and Brain Sciences, Washington University, Campus Box 1125, St. Louis, MO 63130, United States.
E-mail addresses: hawksz@wustl.edu (Z. Hawks), Anna.Hood@cchmc.org (A.M. Hood).
[1] Authors contributed equally to this work.
[2] Present address: Division of Behavioral Medicine and Clinical Psychology, Cincinnati Children's Hospital Medical Center, 3333 Burnet Avenue, MLC 7039, Cincinnati, OH 45229, United States.

https://doi.org/10.1016/j.nicl.2019.101916
Received 4 March 2019; Received in revised form 9 May 2019; Accepted 29 June 2019
Available online 02 July 2019

noted in some individuals with PKU (Christ et al., 2010; Das et al., 2013; Leuzzi et al., 2007, 1993; Manara et al., 2009; Rupp et al., 2001; Scarabino et al., 2009; Thompson et al., 1993). More recently, diffusion tensor imaging (DTI) has been used to study microstructural WM integrity in PKU. DTI studies have identified restricted diffusivity in individuals with PKU across a number of brain regions, including the centrum semiovale, posterior-parietal occipital cortex, prefrontal cortex, optic radiation, putamen, and anterior corpus callosum (Antenor-Dorsey et al., 2013; Christ et al., 2010; Ding et al., 2008; Kono et al., 2005; Peng et al., 2013; Vermathen et al., 2007; White et al., 2013, 2010). Tract based spatial statistics (TBSS) provide convergent evidence for widespread WM compromise in PKU (Antenor-Dorsey et al., 2013; Hawks et al., 2017; Hood et al., 2015).

In contrast, much less is known about gray matter (GM) in PKU. A small body of exploratory research suggests that GM volume may differ between individuals with PKU and neurotypical controls, but the directionality of such effects is unclear. PKU has been associated with decreased GM volume in the parietal lobe, occipital lobe, pons, hippocampus, thalamus, caudate nucleus, and nucleus accumbens (Bodner et al., 2012; Christ et al., 2016; Pérez-Dueñas et al., 2006; Pfaendner et al., 2005). PKU has also been associated with increased brain volume in putamen and the ventral striatum (Bodner et al., 2012; Pérez-Dueñas et al., 2006). Confoundingly, the nucleus accumbens is a substructure of the ventral striatum, yet these regions exhibited opposing group effects (i.e., decreased volume in PKU relative to controls in the nucleus accumbens; increased volume in PKU relative to controls in the ventral striatum). Recent research examining the role of biogenic amines in PKU found a negative correlation between cerebrospinal Phe levels and frontotemporal GM volume, supporting the need for continued Phe control during adulthood to mitigate age-related brain atrophy (Pilotto et al., 2019). Taken together, results strongly motivate further research to elucidate patterns of GM development in PKU.

Moving beyond group differences, little is known regarding the trajectories of WM and GM development in PKU. Likely due to challenges associated with data collection in rare disorders, there have been only two longitudinal studies of brain development in PKU, and both of these studies assessed only WM pathology (Mastrangelo et al., 2015; Nardecchia et al., 2015). Nardecchia et al. found that participants with PKU exhibited normal-appearing WM in early adolescence but WM abnormalities in early adulthood. Relatedly, Mastrangelo et al. retrospectively analyzed serial MRIs from individuals with PKU aged 12 to 37 years and found that the frequency and severity of WM abnormalities increased with age. Of note, these studies used clinician-rated severity scores to describe gross WM abnormalities rather than highly-sensitive DTI approaches.

Methodological differences, small samples sizes, limited longitudinal follow-up, and differing participant characteristics within and across previous studies have hindered attempts to characterize WM and GM development in PKU. We aimed to fill this gap in the literature. To examine WM and GM developmental trajectories, we analyzed DTI and structural MRI data from individuals with PKU and age-matched typically-developing controls. Data were collected at three timepoints over approximately three years. In addition, to determine how the interplay between elevated Phe and WM and GM pathology may influence cognitive outcomes in individuals with PKU, we conducted mediation analyses within our PKU sample. Our study represents the first longitudinal examination of GM in PKU and the first examination of WM and GM within a single sample of individuals with PKU, thereby clarifying the specificity, timing, and cognitive consequences of neural compromise in PKU.

2. Materials and methods

2.1. Participants

Participants with early-and continuously-treated classic PKU (n = 35; 18 males, 17 females) were recruited through metabolic clinics at Washington University in St. Louis (WUSTL) and Oregon Health & Science University (OHSU) (Table 1). All participants were diagnosed in early infancy via newborn screening (Phe > 360 µmol/L) and thereafter placed on restricted Phe diets. The great majority of participants had genetic confirmation of the PAH defect (although not all due to insurance payment denials). Lifetime mean Phe prior to study baseline ranged from 161.1 to 979.8 µmol/L (mean = 399.3, SD = 182.9), and lifetime Phe variability prior to study baseline, measured in standard deviation units, ranged from 75.2 to 452.0 (mean = 217.7, SD = 100.1). WM and GM development in participants with PKU was compared to that of typically developing controls (n = 71; 35 males, 36 females) recruited from St. Louis, Missouri and Portland, Oregon communities. Given our developmental focus, participants were excluded if age at study baseline exceeded 25 years. Participants were also excluded if they reported a history of major medical, psychiatric, or learning disorder unrelated to PKU.

Table 1
Descriptive statistics and IQ for controls and participants with PKU.

	Control		PKU	
Sample Size				
Total	71		35	
Timepoint 1	54		27	
Timepoint 2	45		12	
Timepoint 3	36		22	
	Mean (SD)	Range	Mean (SD)	Range
Age (years)				
Timepoint 1	12.5 (3.5)	7–19	13.0 (4.0)	7–19
Timepoint 2	13 (2.8)	9–19	14.6 (3.5)	10–20
Timepoint 3	14.3 (3.1)	10–21	14.7 (3.5)	10–21
WASI Standard Score				
IQ	115.1 (15.1)	82–143	107.7 (11.0)	86–139

Notes: Controls and participants with PKU were lost to follow-up after timepoints 1 and 2 due to inability to contact, study withdrawal, or failure to attend appointments. SD = standard deviation; WASI = Weschler Abbreviated Scale of Intelligence; IQ = intelligence quotient; WASI scores reflect Timepoint 1 measurements.

2.2. Procedure

Approval for this study was obtained from the institutional review boards at WUSTL and OHSU. Written informed consent was obtained from all participants and/or legal guardians prior to data collection. Referring metabolic clinics provided blood Phe levels over the lifetime based on available medical records. Cognitive and neuroimaging data were collected at each of the three longitudinal timepoints during a session lasting approximately 4 h. The average time elapsed between timepoints 1 and 2 was 1.5 (SD = 0.18, range = 1.3–2.0) years for participants with PKU and 1.6 (SD = 0.12, range = 1.3–1.8) years for controls. The average time elapsed between timepoints 2 and 3 was 1.6 (SD = 0.21, range = 1.1–2.0) years for participants with PKU and 1.5 (SD = 0.14, range = 1.2–1.8) years for controls. Analyses included a total of 196 MRI scans from 35 participants with PKU and 71 controls. Thirty-six participants (14 PKU, 22 control) were scanned twice, and 27 participants (6 PKU, 21 Control) were scanned three times. Some cross-sectional WM and cognitive data reported here were used in previous reports (Hawks et al., 2018; Hood et al., 2016), but findings related to GM and longitudinal trajectories of WM have not been reported previously.

2.3. Imaging data acquisition

Neuroimaging procedures are described in detail by Hood et al. (2016). Briefly, scans were run on a 3.0 T Siemens Trio at OHSU and 1.5 T Siemens Sonata at WUSTL. Structural MRI data included a T1-weighted magnetization prepared rapid acquisition gradient echo

sequence [TR = 1580 ms, TE = 3.93 ms, inversion time of 1000 ms, with isotropic 1.0 × 1.0 × 1.0 mm^3 voxels] and a fast spin echo T2-weighted sequence [TR = 3500 ms, TE = 106 ms, with isotropic 1.0 × 1.0 × 2.0 mm^3 voxels]. DTI data were collected using an echo planar imaging (EPI) sequence acquired 4 times for each participant [TR = 9000 ms, TE = 84 ms (OHSU) and 78 ms (WUSTL), 2.5 mm^3 (OSHU) and 3.0 mm^3 (WUSTL) isotropic voxels, conventional 6 direction encoding with diffusion sensitization of *b*-values = 0 and 1000 s/mm^2]. Total imaging time was approximately 1 h. Due to neuroimaging acquisition complications at OHSU at timepoint 2, MR images from a subset of participants showed poor contrast, necessitating additional exclusions prior to analyses (n = 16; 8 controls, 8 PKU). Available data from these participants at timepoints 1 and 3 were retained.

2.3.1. WM data processing

Four complete DTI datasets were acquired for each participant and were concatenated for the analysis. Diffusion weighted images were registered first to the b = 0 unsensitized image, then to the T2W, then to the best T1W (MPRAGE), and finally to an in-house atlas at WUSTL. Parametric maps were generated for mean diffusivity (MD), axial diffusivity (AD), radial diffusivity (RD), and fractional anisotropy (FA). Whole-brain measures of MD, AD, RD, and FA were computed for each participant by averaging each DTI parameter across the entire WM skeleton using the TBSS method (Smith et al., 2007). Additionally, region of interest (ROI) analyses were used to compare MD between study groups. ROIs were determined using a well-established DTI atlas (Oishi et al., 2008) and verified by a radiologist.

2.3.2. GM data processing

Structural magnetic resonance imaging (MRI) processing and analyses were implemented in FreeSurfer 5.3.0 (https://surfer.nmr.mgh.harvard.edu/) (Fischl, 2012) using the WUSTL Center for High Performance Computing cluster. FreeSurfer was used to parcellate and segment individual participants' anatomical MPRAGE scans at each timepoint in native (non-atlas) space, enabling computation of structural properties for downstream analyses.

Given our concern that neuropathology in PKU might influence automatic segmentation in FreeSurfer, additional attention was taken to ensure data quality. All FreeSurfer segmentations were reviewed for errors (e.g., WM exclusions and dura inclusions) by trained research assistants blinded to participant factors (e.g., group status, age, gender). Errors were manually edited using control points, and edited volumes were reprocessed through the FreeSurfer processing pipeline. Brain volumes were reprocessed up to a maximum of three times, at which point they were excluded from analyses if they did not meet quality control standards. Authors ZH and AH were trained in Human Connectome Project quality control procedures (Marcus et al., 2013) and made final, blinded determinations about data inclusion and exclusion. Exclusions were made at the level of observations (i.e., timepoints) rather than participants. 43 of 239 observations (18%) were excluded prior to analyses due to poor segmentation quality. Corresponding observations were excluded from the DTI dataset to facilitate contrasts between WM and GM.

After data quality was verified, FreeSurfer-generated estimates of GM volume, cortical GM volume, surface area, and cortical thickness were extracted for whole-brain analyses and summed (GM volume, cortical GM volume, surface area) or averaged (cortical thickness) across hemispheres. Additionally, FreeSurfer-generated estimates of volume in the dorsolateral prefrontal cortex (DLPFC), insula, caudate nucleus, putamen, nucleus accumbens, precuneus, supramarginal gyrus, superior parietal lobule, inferior occipital gyrus, posterior transverse collateral sulcus, and parieto-occipital sulcus were extracted for ROI analyses using the Destrieux atlas and summed across hemispheres (Destrieux et al., 2010).

2.4. Index of Phe control

Given that older participants with PKU have accrued longer exposure to elevated Phe compared to younger participants with PKU, we selected mean Phe exposure over the lifetime as our index of Phe control (Hood et al., 2015). This index was based on prior literature modeling exposure to hyperglycemia and hypoglycemia in children with diabetes (Perantie et al., 2007). Like diabetes, PKU is a chronic metabolic illness in which poor dietary management is associated with neural and cognitive consequences (Nardecchia et al., 2015; National Institutes of Health Consensus Development, 2001).

To calculate lifetime Phe exposure, standard (z) scores for lifetime mean Phe and age were computed for each participant based on means and standard deviations of the sample. Lifetime Phe exposure for each participant was then calculated by summing z scores for lifetime Phe and age, producing an approximately normal distribution (mean = 0.15, range = −2.75 to 5.19) where higher scores were indicative of greater exposure. As expected, due to the positive correlation between Phe levels and age, distributional spread was slightly wider than normal (SD = 1.85).

2.5. Executive abilities

An executive abilities composite was created by summing standardized (z) scores from tests of non-verbal strategic processing, verbal strategic processing, and working memory (described in detail in Hood et al., 2016 and Janos et al., 2012). The executive abilities tasks were selected because they have been shown to differentiate participants with PKU from controls (Antenor-Dorsey et al., 2013; DeRoche and Welsh, 2008; Hawks et al., 2017). Briefly, non-verbal strategic processing was assessed using the Matrix Reasoning subtest from the Wechsler Abbreviated Scale of Intelligence (WASI) (Wechsler, 1999), in which participants viewed a series of incomplete matrices and selected one of 5 multiple choice options that best completed each matrix. Total number of correct responses was used in analyses. Verbal strategic processing was assessed using a verbal wordlist learning task in which participants listened to 18 words (with 3 semantic categories) then orally recalled as many words as possible. A ratio reflecting the number of words reported in semantic clusters relative to the total number of words recalled over the five trials was used in analyses. Finally, working memory was assessed using an n-back task with two conditions (location, letter). During the task, participants either pressed a button when the letter presented was in the same location as the letter presented two trials earlier or when the letter presented was identical to the letter presented two trials earlier. The mean number of correct nonresponses, averaged across location and letter conditions, was used in analyses.

2.6. Statistical approach

Analyses were conducted in R (R Core Team, 2017) using the package *lme4* for nested modeling (Bates et al., 2015) and *psych* for mediation modeling (Revelle, 2018).

2.6.1. Sample characteristics

Independent samples, Chi-squared, and Fisher Exact tests were used to assess demographic group differences. Hierarchical linear modeling (HLM) was used to assess group differences in intelligence quotient (IQ), accounting for longitudinal dependencies in the data.

2.6.2. Developmental trajectories

GM and WM developmental trajectories in PKU and control groups were analyzed using HLM. HLM is an advanced regression technique that accounts for shared variance in hierarchically-structured (i.e., nested) data (Woltman et al., 2012). In the present study, timepoints were nested within individuals. Unlike univariate analyses, HLM

utilizes the entire sample to optimize prediction at a given age. Thus, the method was robust to the wide age range under study, providing information about brain development across childhood and adolescence without sacrificing statistical power. Age was a Level 1 variable in our models, and group was a Level 2 variable.

$$\begin{aligned} \textit{Level 1:}\quad & Y_{ij} = \beta_{0i} + \beta_{1i}(Age)_{ij} + e_{ij} \\ \textit{Level 2:}\quad & \beta_{0i} = \gamma_{00} + \gamma_{01}(Group)_i + \mu_{0i} \\ & \beta_{1i} = \gamma_{10} + \gamma_{11}(Group)_i \end{aligned}$$

WM dependent variables included 4 whole-brain measures (MD, AD, RD, FA). Seven WM ROIs were also selected on the basis of prior significant findings in cross-sectional studies of PKU (Antenor-Dorsey et al., 2013; Hood et al., 2015; White et al., 2013). These included the optic radiation, hippocampus, putamen, posterior-parietal occipital cortex (PPO), corpus callosum (CC), centrum semiovale (CSO), and prefrontal cortex WM (PFC-WM). To limit the number of comparisons, we selected MD for ROI analyses because it has been most consistently implicated (relative to RD, AD, and FA) in DTI studies of PKU (e.g., Antenor-Dorsey et al., 2013).

GM dependent variables included 4 whole-brain measures (total GM volume, cortical GM volume, total surface area, and average cortical thickness). Eleven GM ROIs were also selected on the basis of prior significant findings in cross-sectional studies of PKU (e.g., putamen and parieto-occipital lobes) (Bodner et al., 2012; Christ et al., 2016) and/or to map onto WM ROIs (e.g., PFC structures). GM ROIs included the dorsolateral prefrontal cortex (DLPFC), insula, caudate nucleus, putamen, nucleus accumbens, precuneus, supramarginal gyrus, superior parietal lobule, inferior occipital gyrus, posterior transverse collateral sulcus, and parieto-occipital sulcus.

For each WM and GM dependent variable, we ran a linear model to examine the effects of age (grand-mean centered at 13.4 years), group, and their cross-level (age × group) interaction. Given previous literature regarding developmental trajectories (Wierenga et al., 2014b), quadratic and cubic effects for age were also examined. To avoid overfitting, preferred models were selected to minimize the Bayesian Information Criterion (BIC). Holm's correction was used to adjust for multiple comparisons (Holm, 1979).

2.6.3. Longitudinal mediation analyses

Mediation analyses examined whether brain measures influenced the relationship between lifetime Phe exposure and executive abilities. Specifically, we aimed to determine how relationships among these variables may unfold over time. To this end, we required that each participant contribute three data points to mediation models: (1) lifetime Phe exposure, calculated using all available blood Phe levels preceding study baseline (i.e., the timepoint at which data were first collected from that participant); (2) neuroimaging data, collected at study baseline; and (3) executive data, collected at a visit subsequent to study baseline. In contrast with trajectory analyses, which included all available neuroimaging data, mediation analyses included a single neuroimaging scan from each participant.

Mediation was implemented using a bootstrapping approach (10,000 re-samplings), which is a non-parametric resampling procedure for the assessment of indirect effects (Preacher and Hayes, 2008). Significant indirect effects can occur in the absence of significant total or direct effects. In the present analyses, the independent variable was lifetime Phe exposure, the dependent variable was the executive abilities composite, and the predicted mediators were brain measures (i.e., whole-brain and regional WM and GM). Variables were standardized prior to analyses for ease of comparing mediation effects. Indirect effects were considered significant when the 95% confidence interval (CI) excluded zero.

3. Results

3.1. Sample characteristics

There were no significant differences between participants with PKU and controls with respect to age, gender, race (White vs. non-White), or ethnicity ($ps > 0.05$). As is often the case in studies of PKU (Waisbren et al., 2007), estimated IQ was significantly lower among participants with PKU relative to controls ($\gamma = -7.3$, $SE = 2.7$, $p < .05$).

3.2. Whole-brain analyses

We began analyses at the broadest level by examining developmental trajectories of 4 whole-brain measures of average WM integrity (MD, AD, RD, and FA) and 4 whole brain measures of GM structure (cortical GM volume, total surface area, and average cortical thickness). All significant results reported survived Holm's correction for multiple comparisons. A linear model for age was consistently preferred over quadratic and cubic models (see Supplementary Table 1).

3.2.1. WM analyses

Analyses examined the effects of age, group, and age × group on MD, AD, RD, and FA. For 3 of 4 whole-brain WM measures (MD, RD, FA), we found a significant main effect of age, indicating that average MD and RD decreased whereas average FA increased as participants got older (accounting for group and the age × group interaction; $ps < 0.001$). For 3 of 4 whole-brain WM measures (MD, RD, FA), we found a significant main effect of group, indicating that participants with PKU exhibited reduced MD and RD and increased FA compared to controls (accounting for age and the age × group interaction; $ps < 0.001$). For 2 of 4 whole-brain WM measures (MD, AD), we found significant age × group interactions ($ps < 0.001$), indicating that MD and AD decreased more as a function of age in participants with PKU relative to controls. Overall, these results indicate robust, widespread WM differences between participants with PKU and controls, such that participants with PKU have poorer WM integrity relative to controls, which worsens as they age (see Fig. 1 and Supplementary Table 2).

3.2.2. GM analyses

Analyses examined the effects of age, group, and age × group on total GM volume, cortical GM volume, total surface area, and average cortical thickness. For all 4 measures of whole-brain GM, we found a significant main effect of age, indicating that whole-brain GM decreased as participants got older regardless of group status ($ps < 0.001$). In stark contrast with our whole-brain WM results, there were no significant effects of group or interactions between age and group for whole-brain GM (see Fig. 2 and Supplementary Table 3).

3.3. Region of interest (ROI) analyses

As our next step, we modeled development in our 7 WM and 11 GM ROIs. MD was used for all WM ROI analyses and volume was used for all GM ROI analyses. ROI analyses provided specificity with respect to the location and magnitude of neural differences between participants with PKU and controls. All significant results reported survived Holm's correction for multiple comparisons. A linear model for age was consistently preferred over quadratic and cubic models (see Supplementary Table 1).

3.3.1. WM analyses

Analyses examined the effects of age, group, and age × group on MD in 7 WM ROIs. In a minority of WM ROIs (2 of 7: PPO and CSO), we found a significant main effect of age ($p < .001$), indicating that MD did not generally decrease as participants got older (accounting for group and the age × group interaction; $ps > 0.05$). In 3 of 7 WM ROIs

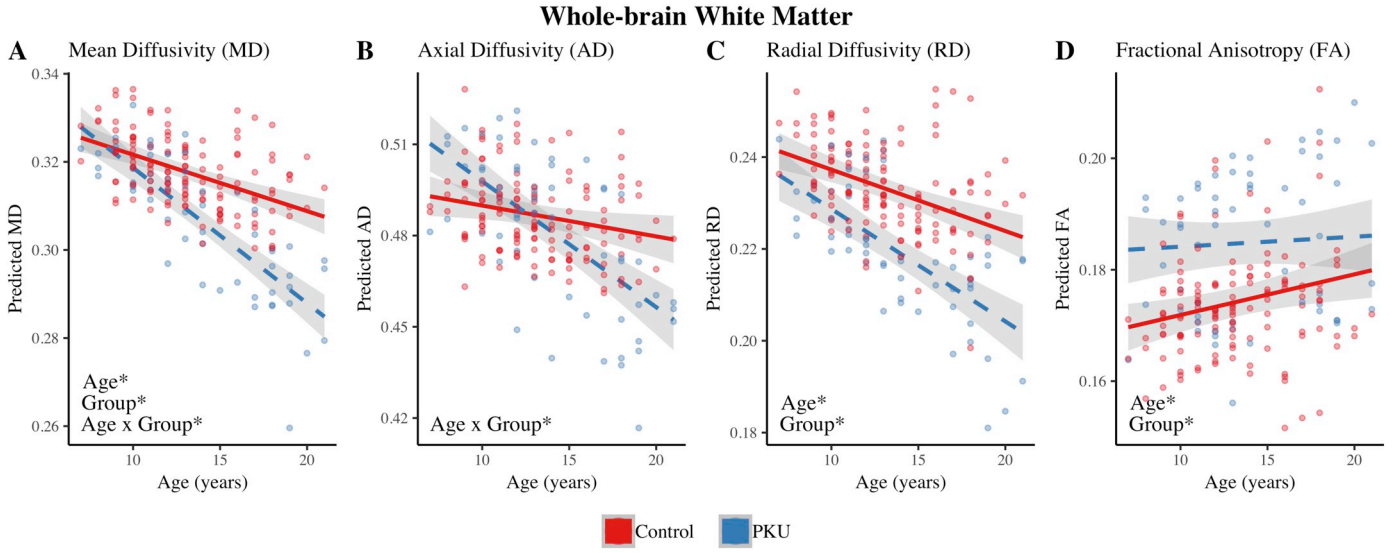

Fig. 1. Developmental trajectories of whole-brain WM integrity in participants with PKU (dotted lines) compared to controls (solid lines). Significant effects of age, group, and age × group are denoted by asterisks (*) in the bottom left corner of each graph. Shaded bands represent 95% confidence intervals.

(PPO, CC, and CSO), we found a significant main effect of group, indicating that participants with PKU often exhibited decreased MD relative to controls (accounting for age and the age × group interaction; *ps* < 0.01). Finally, in a majority of WM ROIs (5 of 7: optic radiation, hippocampus, PPO, CC, and CSO), we found significant age × group interactions (*ps* < 0.01), indicating that MD decreased more as a function of age in participants with PKU relative to controls. Overall, results related to WM once again indicated widespread WM differences between participants with PKU and controls (see Fig. 3 and Supplementary Table 4), with worsening WM integrity as individuals with PKU aged.

3.3.2. GM analyses

Analyses examined the effects of age, group, and age × group on GM volume in 11 ROIs. In a majority of ROIs (8 of 11: DLPFC, caudate nucleus, nucleus accumbens, precuneus, supramarginal gyrus, superior parietal lobule, and parieto-occipital sulcus), we found a significant main effect of age, indicating that ROI volume generally decreased as participants got older regardless of group status (*p* < .01). Similar to whole-brain GM results and in contrast with WM results, there were no significant effects of group or interactions between age and group (*ps* > 0.05; see Supplementary Table 5).

3.4. Mediation

Given the well-documented executive dysfunction in participants with PKU (Araujo et al., 2009; Banerjee et al., 2011; Christ et al., 2006; Huijbregts et al., 2013), we explored whether brain measures that distinguished participants with PKU from controls also mediated the relationship between lifetime Phe exposure and executive abilities in our cohort of participants with PKU (Hood et al., 2014). To this end, we conducted mediation analyses, focusing our analyses on WM measures for which developmental trajectories differed between participants with PKU and controls (i.e., significant effects of group and/or age × group; see sections 3.2.1. and 3.3.1). No GM measures were included in mediation analyses because none yielded significant group or

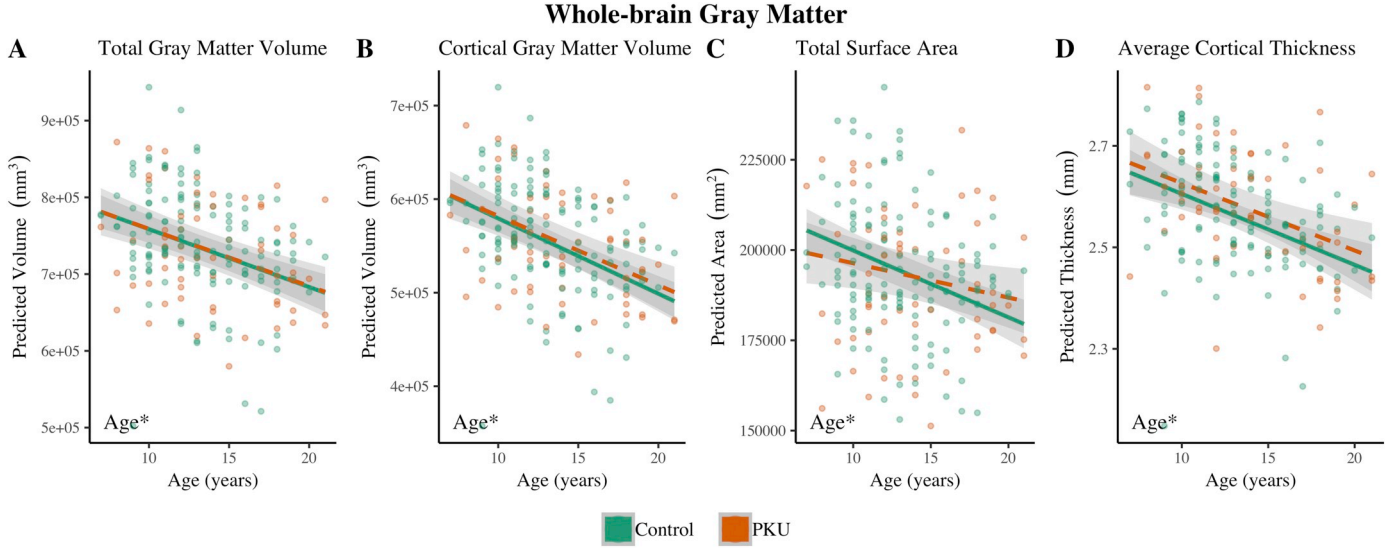

Fig. 2. Developmental trajectories of whole-brain GM in participants with PKU (dotted lines) compared to controls (solid lines). Significant effects of age, denoted by asterisks (*), were consistently observed. The main effect of group and the age × group interaction never reached significance. Shaded bands represent 95% confidence intervals.

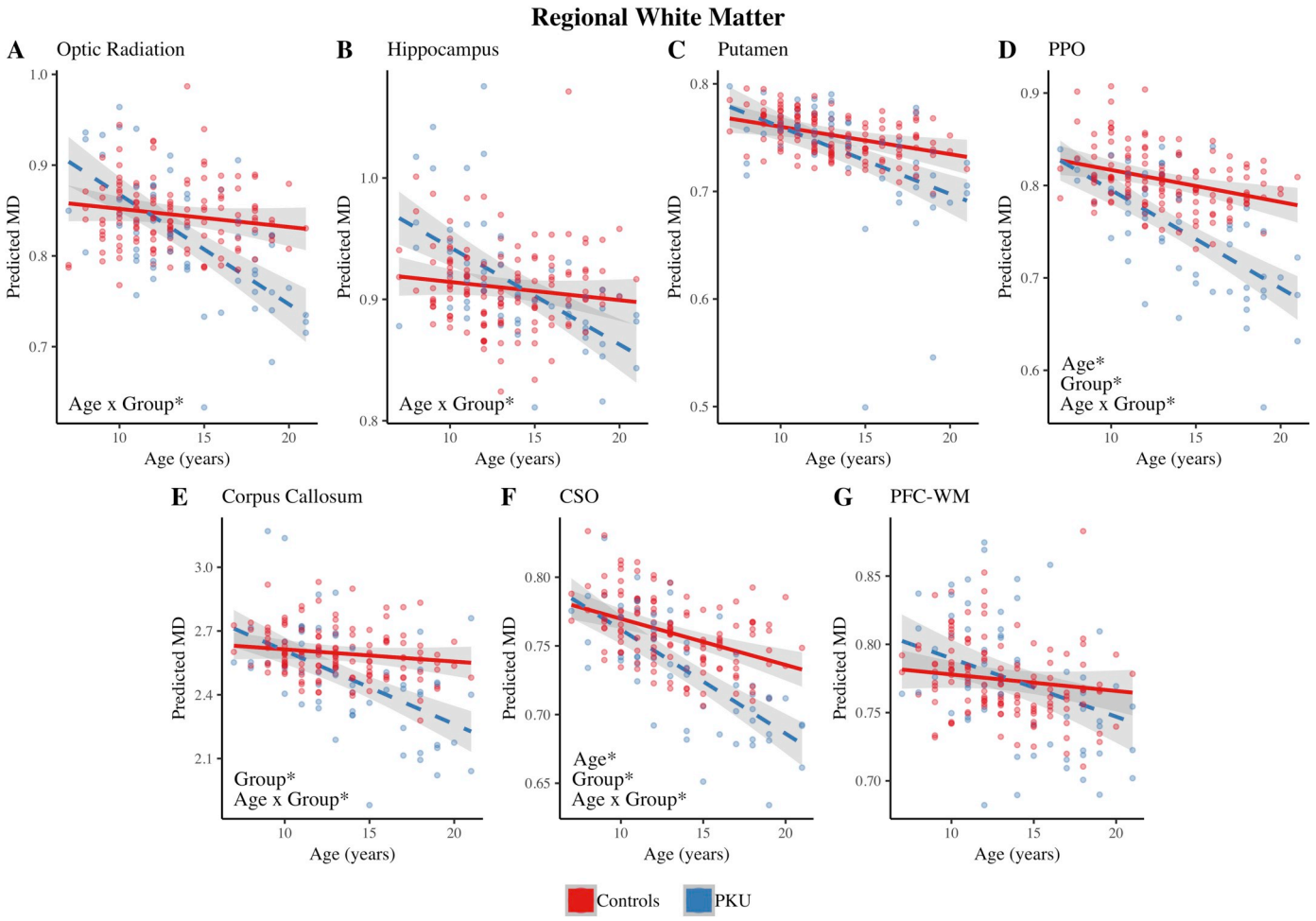

Fig. 3. Developmental trajectories of regional WM integrity in participants with PKU (dotted lines) compared to controls (solid lines). Significant effects of age, group, and age × group are denoted by asterisks (*) in the bottom left corner of each graph. Shaded bands represent 95% confidence intervals.

age × group effects.

Of the 9 mediation analyses conducted, 3 yielded statistically significant indirect effects. Specifically, the indirect effect of lifetime Phe exposure on executive abilities was significant for whole-brain MD (95% CI = [−1.91, −0.04]), MD in the CC (95% CI = [−0.85, −0.02]), and MD in the CSO (95% CI = [−1.21, −0.19]) (see Table 2). All significant indirect effects occurred in the context of significant direct effects (weight *c′*) and non-significant total effects (weight *c*). These results indicated that whole-brain MD, MD in the CC, and MD in the CSO mediate the relationship between lifetime Phe exposure and executive abilities in individuals with PKU.

Table 2
Whole-brain and regional WM as mediators of the relationship between lifetime Phe exposure and executive abilities.

Mediator	*a*	*b*	*c*	*c′*	Indirect effect		R^2
					Estimate (SE)	95% CI	
Whole-Brain WM							
MD	−0.88 (0.12)*	0.92 (0.41)*	0.46 (0.22)	1.27 (0.41)*	−0.86 (0.46)	[−1.91, −0.04]	0.41
AD	−0.84 (0.14)*	0.40 (0.41)	0.46 (0.22)	0.80 (0.41)	−0.31 (0.31)	[−0.90, 0.31]	0.26
RD	−0.67 (0.19)*	0.43 (0.29)	0.46 (0.22)	0.75 (0.29)*	−0.29 (0.22)	[−0.79, 0.08]	0.32
FA	0.03 (0.25)	−0.18 (0.22)	0.46 (0.22)	0.47 (0.22)	−0.03 (0.07)	[−0.22, 0.07]	0.25
Regional WM							
Optic Radiation	−0.75 (0.15)*	−0.35 (0.32)	0.44 (0.21)	0.18 (0.32)	0.26 (0.23)	[−0.17, 0.73]	0.25
Hippocampus	−0.75 (0.16)*	0.14 (0.32)	0.44 (0.21)	0.55 (0.32)	−0.10 (0.27)	[−0.62, 0.45]	0.21
PPO	−0.80 (0.14)*	0.21 (0.36)	0.44 (0.21)	0.61 (0.36)	−0.16 (0.28)	[−0.68, 0.45]	0.21
CC	−0.55 (0.20)*	0.43 (0.24)	0.44 (0.21)	0.68 (0.24)*	−0.30 (0.22)	[−0.85, −0.02]	0.33
CSO	−0.82 (0.13)*	0.91 (0.31)*	0.44 (0.21)	1.2 (0.31)*	−0.71 (0.25)	[−1.21, −0.19]	0.47

Notes: Significant indirect effects (bolded) do not include zero within the 95% CI. SE = standard error; CI = confidence interval; WM = white matter; MD, AD, and RD = mean, axial, and radial diffusivity, respectively; FA = fractional anisotropy; PPO = posterior parietal occipital cortex; CC = corpus callosum; CSO = centrum semiovale.

* $p < .05$.

4. Discussion

The present study is the first to investigate longitudinal developmental trajectories of GM in children and young adults with PKU, and it is the first to examine trajectories of GM and WM within a single sample of individuals with PKU. With respect to WM, results indicated widespread differences between individuals with PKU and controls: individuals with PKU generally exhibited decreased MD, AD, and RD, but increased FA. These group differences were observed at whole-brain as well as regional-brain (ROI) levels and were frequently exacerbated by increasing age. Notably, numerous past studies have observed little to no difference in FA between individuals with PKU and controls (e.g., Antenor-Dorsey et al., 2013; Ding et al., 2008; Peng et al., 2013; Vermathen et al., 2007; White et al., 2010). This discrepancy may be attributable to differences in DTI processing (ROI vs. whole-brain), study design (longitudinal vs. cross-sectional), sample characteristics (adolescent vs. adult), and/or sample size (additional participants increase statistical power to detect significant effects).

In marked contrast with WM trajectories, GM trajectories did not differ between individuals with PKU and controls. Specifically, across *all* models testing the effects of age and group on GM structures, the main effect of group and the interaction between age and group were never statistically significant, nor were their effect sizes appreciable. This pattern suggests that our results cannot be accounted for by low power and instead reflect comparable development of GM in individuals with PKU and controls. Significant main effects of age indicated that, irrespective of group status, brain volume, surface area, and cortical thickness tended to decrease as age increased, patterns that are generally consistent with prior reports of normative brain development (e.g., Wierenga et al., 2014b, 2014a).

To link neural substrates to treatment compliance (i.e., Phe control) and cognitive outcome within our PKU sample, we conducted mediation analyses. Analyses focused on WM structures in which trajectory analyses indicated significant effects of group and/or age × group. We found that whole-brain MD and regional MD in the CC and CSO mediated the relationship between Phe control and executive abilities. These results provide empirical support for a plausible neurobiological mechanism by which Phe control may influence cognition in individuals with PKU. Specifically, poorer Phe control may disrupt white matter integrity, with negative consequences for executive functioning (Anderson and Leuzzi, 2009; Christ et al., 2010; Joseph and Dyer, 2003). However, in 6 of 9 mediation analyses, we failed to observe significant indirect effects. It is possible that our executive composite lacked sufficient specificity to detect indirect effects relating to individual executive abilities (e.g., working memory). Indeed, prior cross-sectional research by Hood et al. (2016) modeled distinct executive abilities individually and identified indirect effects of MD in both the CSO and PPO in adolescents with PKU. Alternatively, it is possible that executive abilities are highly susceptible to recent Phe levels, in which case a different index of Phe control (e.g., Phe measured closest to the time of testing or mean Phe in the year prior to testing) may increase the sensitivity of mediation analyses. In future studies, it will be of interest to explore the time-course of relationships among Phe control, white matter integrity, and cognition in both executive and non-executive domains (e.g., processing speed).

Taken together, findings from the present study indicate that PKU-related neuropathology is more prominent in WM compared to GM structures. This was indicated by the frequency and magnitude of group and age × group effects in WM, as well as the consistency of null results (for group and age × group) in GM. Although extant research has consistently demonstrated widespread WM compromise in individuals with PKU (Hood et al., 2015; Peng et al., 2013; Vermathen et al., 2007; White et al., 2010), research on GM structures is more limited (Christ et al., 2016; Pfaendner et al., 2005). The relative lack of research necessitated an exploratory (albeit hypothesis-driven) approach to GM ROI selection in the present study. As such, we cannot rule out the possibility that GM pathology exists elsewhere in the brain, as has been found previously in cross-sectional analyses (Bodner et al., 2012). Nor can we rule out the possibility that GM pathology may emerge in adulthood, when Phe control tends to worsen and lifetime Phe exposure tends to increase. Indeed, our sample was younger (mean age = 13.0 years at timepoint 1) and exhibited better dietary control (lifetime mean Phe = 399.3 μmol/L) compared to published samples in which significant group differences in GM volume have been obtained (e.g., mean age = 22 years, lifetime mean Phe = 610 μmol/L in Bodner et al., 2012 and mean age = 21 years, lifetime mean Phe = 597 μmol/L in Christ et al., 2016; Phe levels conveyed via personal communication). Lastly, the present study did not measure, and therefore cannot speak to, potential functional differences in the GM (e.g., functional MRI, functional connectivity MRI) between individuals with PKU and controls. Despite having one of the largest samples of any PKU neuroimaging study to date, we acknowledge that we are underpowered to completely support the null hypothesis, and fine-grained GM differences may yet exist between individuals with PKU and controls. Notwithstanding, the magnitude of any such differences appears to pale in comparison to the scope of WM compromise.

Finally, it is interesting to consider why WM became increasingly compromised as individuals with PKU grew older, despite the fact that all participants in our sample were early-and-continuously treated with low Phe diets since infancy. PKU requires lifelong, strict adherence to an unpalatable and complicated diet. As children with PKU progress through adolescence and gain independence, dietary compliance often worsens (Brown and Lichter-Konecki, 2016), which may contribute to WM pathology. It is also possible that lasting changes in brain maturation are seeded shortly after birth, prior to treatment implementation. Future lifespan studies of PKU will be necessary to disambiguate these possibilities. Future studies will also be necessary to determine why PKU appears to differentially effect WM and GM.

5. Conclusion

The present study was the first to assess WM and GM developmental trajectories within a single cohort of children and young adults with PKU. Our study yielded several important findings. First, longitudinal analyses indicated that there was widespread WM compromise in individuals with PKU, which was exacerbated by increasing age. Second, widespread WM compromise in PKU occurred in the absence of whole-brain and/or regional GM pathology. Finally, WM compromise mediated the relationship between treatment compliance (i.e., Phe control) and executive abilities, suggesting a possible neural mechanism to explain the significant cognitive sequelae seen in individuals with PKU. Our results make significant contributions to the literature regarding neurodevelopment in PKU, as they clarify the specificity, timing, and cognitive consequences of whole-brain and focal WM compromise. They also contribute to a growing view emphasizing the importance of lifelong dietary control in PKU (Hawks et al., 2018; Hood et al., 2015, 2014; Pilotto et al., 2019; Van Wegberg et al., 2017).

Acknowledgements

The authors wish to thank the participants and families who generously participated in our research. We also thank Suzin Blankenship and Laurie Sprietsma for their contributions to study management, and Annie Lee, Maggie Clapp, Kelly Reger, Devante Morgan, and Amanda Namchuk for their assistance with data processing. Additionally, we would like to thank the physicians and staff of Washington University and Oregon Health & Science University who generously contributed to the study through recruitment and phenylalanine monitoring.

Funding sources

This research was supported by the National Institute of Child

Health and Human Development (R01HD044901 and U54HD087011). Computations were performed using facilities of the Washington University Center for High Performance Computing, which were partially provided through NIH grant S10 OD018091. During the study period, Anna Hood was supported in part by the National Heart, Lung, and Blood Institute (1F31HL134314-01) and Dov Lerman-Sinkoff was supported in part by the National Institute of Mental Health (F30MH109294).

Declaration of Competing Interest

Zoë Hawks, Anna Hood, Jerrel Rutlin, Joshua Shimony, and Daniel Lagoni declare that they have no conflicts of interest. Desirée White and Dorothy Grange have received research grants from BioMarin Pharmaceutical Inc. and have served as consultants for BioMarin Pharmaceutical Inc. Dov Lerman-Sinkoff has received payment from an unrelated pharmaceutical company for use of his pet in veterinary product advertisements.

Appendix A. Supplementary data

Supplementary data to this article can be found online at https://doi.org/10.1016/j.nicl.2019.101916.

References

Anderson, P.J., Leuzzi, V., 2009. White matter pathology in phenylketonuria. Mol. Genet. Metab. 99, S3–S9. https://doi.org/10.1016/j.ymgme.2009.10.005.

Anderson, P.J., Wood, S.J., Francis, D.E., Coleman, L., Anderson, V., Boneh, A., 2007. Are neuropsychological impairments in children with early-treated phenylketonuria (PKU) related to white matter abnormalities or elevated phenylalanine levels? Dev. Neuropsychol. Neuro Cogn. Conseq. White Matter Injury Child. 32, 645–668.

Antenor-Dorsey, J.A.V., Hershey, T., Rutlin, J., Shimony, J.S., McKinstry, R.C., Grange, D.K., Christ, S.E., White, D.A., 2013. White matter integrity and executive abilities in individuals with phenylketonuria. Mol. Genet. Metab. 109, 125–131. https://doi.org/10.1016/j.ymgme.2013.03.020.

Araujo, G.C., Christ, S.E., Steiner, R.D., Grange, D.K., Nardos, B., McKinstry, R.C., White, D. a, 2009. Response monitoring in children with phenylketonuria. Neuropsychology 23, 130–134. https://doi.org/10.1037/a0013488.

Banerjee, P., Grange, D.K., Steiner, R.D., White, D. a, 2011. Executive strategic processing during verbal fluency performance in children with phenylketonuria. Child. Neuropsychol. 17, 105–117. https://doi.org/10.1080/09297049.2010.525502.

Bates, D., Maechler, M., Bolker, B., Walker, S., 2015. Fitting linear mixed-effects models using lme4. J. Stat. Softw. 67, 1–48. https://doi.org/10.18637/jss.v067.i01.

Bodner, K.E., Aldridge, K., Moffitt, A.J., Peck, D., White, D.A., Christ, S.E., 2012. A volumetric study of basal ganglia structures in individuals with early-treated phenylketonuria. Mol. Genet. Metab. 107, 302–307. https://doi.org/10.1016/j.ymgme.2012.08.007.

Brown, C.S., Lichter-Konecki, U., 2016. Phenylketonuria (PKU): a problem solved? Mol. Genet. Metab. Rep. 6, 8–12. https://doi.org/10.1016/j.ymgmr.2015.12.004.

Christ, S.E., Steiner, R.D., Grange, D.K., Abrams, R. a, White, D. a, 2006. Inhibitory control in children with phenylketonuria. Dev. Neuropsychol. 30, 845–864. https://doi.org/10.1207/s15326942dn3003_5.

Christ, S.E., Huijbregts, S.C.J., de Sonneville, L.M.J., White, D.A., 2010. Executive function in early-treated phenylketonuria: profile and underlying mechanisms. Mol. Genet. Metab. 99, S22–S32 Supple.

Christ, S.E., Price, M.H., Bodner, K.E., Saville, C., Moffitt, A.J., Peck, D., 2016. Morphometric analysis of gray matter integrity in individuals with early-treated phenylketonuria. Mol. Genet. Metab. https://doi.org/10.1016/j.ymgme.2016.02.004.

Das, A.M., Goedecke, K., Meyer, U., Kanzelmeyer, N., Koch, S., Illsinger, S., Lücke, T., Hartmann, H., Lange, K., Lanfermann, H., 2013. Dietary Habits and Metabolic Control in Adolescents and Young Adults With Phenylketonuria: Self-Imposed Protein Restriction may be Harmful.

DeRoche, K., Welsh, M., 2008. Twenty-five years of research on neurocognitive outcomes in early-treated phenylketonuria: intelligence and executive function. Dev. Neuropsychol. 33, 474–504. https://doi.org/10.1080/87565640802101482.

Destrieux, C., Fischl, B., Dale, A., Halgren, E., 2010. Automatic parcellation of human cortical gyri and sulci using standard anatomical nomenclature. Neuroimage 53. https://doi.org/10.1016/j.neuroimage.2010.06.010.Automatic.

Ding, X., Fiehler, J., Kohlschütter, B., Wittkugel, O., Grzyska, U., Zeumer, H., Ullrich, K., 2008. MRI abnormalities in normal-appearing brain tissue of treated adult PKU patients. J. Magn. Reson. Imaging 27, 998–1004.

Dyer, C.A., 1999. Pathophysiology of phenylketonuria. Ment. Retard. Dev. Disabil. Res. Rev. 5, 104–112.

Fischl, B., 2012. FreeSurfer. Neuroimage 62, 774–781. https://doi.org/10.1016/j.neuroimage.2012.01.021.FreeSurfer.

Hardelid, P., Cortina-Borja, M., Munro, A., Jones, H., Cleary, M., Champion, M.P., Foo, Y., Scriver, C.R., Dezateux, C., 2008. The birth prevalence of PKU in populations of European, south Asian and sub-Saharan African ancestry living in South East England. Ann. Hum. Genet. 72, 65–71.

Hawks, Z., Shimony, J., Rutlin, J., Grange, D.K., Christ, S.E., White, D.A., 2017. Pretreatment cognitive and neural differences between sapropterin dihydrochloride responders and non-responders with phenylketonuria. Mol. Genet. Metab. Rep. https://doi.org/10.1016/j.ymgmr.2017.01.013.

Hawks, Z.W., Strube, M.J., Johnson, N.X., Grange, D.K., White, D.A., 2018. Developmental trajectories of executive and verbal processes in children with phenylketonuria. Dev. Neuropsychol. 43, 207–218. https://doi.org/10.1080/87565641.2018.1438439.

Holm, S., 1979. A simple sequentially rejective multiple test procedure. Scand. J. Stat. 6, 65–70.

Hood, A., Grange, D.K., Christ, S.E., Steiner, R., White, D.A., 2014. Variability in phenylalanine control predicts IQ and executive abilities in children with phenylketonuria. Mol. Genet. Metab. 111, 445–451. https://doi.org/10.1016/j.ymgme.2014.01.012.

Hood, A., Antenor-Dorsey, J.A.V., Rutlin, J., Hershey, T., Shimony, J.S., McKinstry, R.C., Grange, D.K., Christ, S.E., Steiner, R., White, D.A., 2015. Prolonged exposure to high and variable phenylalanine levels over the lifetime predicts brain white matter integrity in children with phenylketonuria. Mol. Genet. Metab. 114, 19–24. https://doi.org/10.1016/j.ymgme.2014.11.007.

Hood, A., Rutlin, J., Shimony, J.S., Grange, D.K., White, D.A., 2016. Rutlin J citation Brain White Matter Integrity Mediates the Relationship Between Phenylalanine Control and Executive Abilities in Children With Phenylketonuria. JIMD Reports 33, 41–47.

Huijbregts, S.C.J., Gassió, R., Campistol, J., 2013. Executive functioning in context: relevance for treatment and monitoring of phenylketonuria. Mol. Genet. Metab. 110, S25–S30. https://doi.org/10.1016/j.ymgme.2013.10.001.

Jahja, R., van Spronsen, F.J., de Sonneville, L.M.J., van der Meere, J.J., Bosch, A.M., Hollak, C.E.M., Rubio-Gozalbo, M.E., Brouwers, M.C.G.J., Hofstede, F.C., de Vries, M.C., Janssen, M.C.H., van der Ploeg, A.T., Langendonk, J.G., Huijbregts, S.C.J., 2017. Long-term follow-up of cognition and mental health in adult phenylketonuria: a PKU-COBESO study. Behav. Genet. 47, 486–497. https://doi.org/10.1007/s10519-017-9863-1.

Janos, A.L., Grange, D.K., Steiner, R.D., White, D.a., 2012. Processing speed and executive abilities in children with phenylketonuria. Neuropsychology 26, 735–743. https://doi.org/10.1037/a0029419.

Joseph, B., Dyer, C.A., 2003. Relationship between Myelin Production and Dopamine Synthesis in the PKU Mouse Brain. pp. 615–626. https://doi.org/10.1046/j.1471-4159.2003.01887.x.

Kono, K., Okano, Y., Nakayama, K., Hase, Y., Minamikawa, S., Ozawa, N., Yokote, H., Inoue, Y., 2005. Diffusion-weighted MR imaging in patients with phenylketonuria: relationship between serum phenylalanine levels and ADC values in cerebral White Matter1. Radiology 236, 630–636.

Leuzzi, V., Gualdi, G.F., Fabbrizi, F., Trasimeni, G., Di Biasi, C., Antonozzi, I., 1993. Neuroradiological (MRI) abnormalities in phenylketonuric subjects: clinical and biochemical correlations. Neuropediatrics 24, 302–306.

Leuzzi, V., Tosetti, M., Montanaro, D., Carducci, C., Artiola, C., Antonozzi, I., Burroni, M., Carnevale, F., Chiarotti, F., Popolizio, T., 2007. The pathogenesis of the white matter abnormalities in phenylketonuria. A multimodal 3.0 tesla MRI and magnetic resonance spectroscopy (1H MRS) study. J. Inherit. Metab. Dis. 30, 209–216.

Manara, R., Burlina, A.P., Citton, V., Ermani, M., Vespignani, F., Carollo, C., Burlina, A.B., 2009. Brain MRI diffusion-weighted imaging in patients with classical phenylketonuria. Neuroradiology 51, 803–812.

Marcus, D.S., Harms, M.P., Snyder, A.Z., Jenkinson, M., Anthony, J., Glasser, M.F., Barch, D.M., Archie, K.A., Burgess, G.C., Ramaratnam, M., Hodge, M., Horton, W., Herrick, R., Olsen, T., Mckay, M., House, M., Hileman, M., Reid, E., Harwell, J., Schindler, J., Elam, J.S., Curtiss, S.W., Essen, D.C. Van, 2013. Human Connectome Project Informatics: quality control, database services, and data visualization. Neuroimage 202–219. https://doi.org/10.1016/j.neuroimage.2013.05.077.Human.

Mastrangelo, M., Chiarotti, F., Berillo, L., Caputi, C., Carducci, C., Di Biasi, C., Manti, F., Nardecchia, F., Leuzzi, V., 2015. The outcome of white matter abnormalities in early treated phenylketonuric patients: a retrospective longitudinal long-term study. Mol. Genet. Metab. 116, 171–177.

Nardecchia, F., Manti, F., Chiarotti, F., Carducci, C., Carducci, C., Leuzzi, V., 2015. Neurocognitive and neuroimaging outcome of early treated young adult PKU patients: a longitudinal study. Mol. Genet. Metab. 115, 84–90.

National Institutes of Health Consensus Development Panel, 2001. National institutes of health consensus development conference statement: phenylketonuria: screening and management, October 16–18, 2000. Pediatrics 108 (4), 972–982.

Oishi, K., Zilles, K., Amunts, K., Faria, A., Jiang, H., Li, X., Akhter, K., Hua, K., Woods, R., Toga, A.W., Pike, G.B., Rosa-, P., Evans, A., Zhang, J., Huang, H., Miller, M.I., Van, P.C.M., Mazziotta, J., Mori, S., Brain, F., 2008. Human brain white matter atlas: identification and assignment of common anatomical structures in superficial white matter. Neuroimage 43, 447–457. https://doi.org/10.1016/j.neuroimage.2008.07.009.Human.

Peng, H., Peck, D., White, D.A., Christ, S.E., 2013. Tract-based evaluation of white matter damage in individuals with early-treated phenylketonuria. J. Inherit. Metab. Dis. 1–7.

Perantie, D.C., Wu, J., Koller, J.M., Lim, A., Warren, S.L., Black, K.J., Sadler, M., White, N.H., Hershey, T., 2007. Regional brain volume differences associated with hyperglycemia and severe hypoglycemia in youth with type 1 diabetes. Diabetes Care 30, 2331–2337. https://doi.org/10.2337/dc07-0351.

Pérez-Dueñas, B., Pujol, J., Soriano-Mas, C., Ortiz, H., Artuch, R., Vilaseca, M.A., Campistol, J., 2006. Global and regional volume changes in the brains of patients with phenylketonuria. Neurology 66, 1074–1078. https://doi.org/10.1212/01.wnl.

0000204415.39853.4a.
Pfaendner, N.H., Reuner, G., Pietz, J., Jost, G., Rating, D., Magnotta, V.A., Mohr, A., Kress, B., Sartor, K., Hähnel, S., 2005. MR imaging-based volumetry in patients with early-treated phenylketonuria. Am. J. Neuroradiol. 26, 1681–1685 doi:26/7/1681 [pii].
Pilotto, A., Blau, N., Leks, E., Schulte, C., Deuschl, C., Zipser, C., Piel, D., Freisinger, P., Gramer, G., Kölker, S., Haas, D., Burgard, P., Nawroth, P., Georg, H., Scheffler, K., Berg, D., Trefz, F., 2019. Cerebrospinal fluid biogenic amines depletion and brain atrophy in adult patients with phenylketonuria. J. Inherit. Metab. Dis. 398–406. https://doi.org/10.1002/jimd.12049.
Preacher, K., Hayes, A., 2008. Asymptotic and resampling strategies for assessing and comparing indirect effects in multiple mediator models. Behav. Res. Methods 40, 879–891. https://doi.org/10.3758/BRM.40.3.879.
R Core Team, 2017. R: A Language and Environment for Statistical Computing.
Revelle, W., 2018. psych: Procedures for Personality and Psychological Research.
Rupp, A., Kreis, R., Zschocke, J., Slotboom, J., Boesch, C., 2001. Variability of blood–brain ratios of phenylalanine in typical patients with phenylketonuria. J. Cereb. Blood Flow Metab. 21, 276–284.
Scarabino, T., Popolizio, T., Tosetti, M., Montanaro, D., Giannatempo, G.M., Terlizzi, R., Pollice, S., Maiorana, A., Maggialetti, N., Carriero, A., 2009. Phenylketonuria: white-matter changes assessed by 3.0-T magnetic resonance (MR) imaging, MR spectroscopy and MR diffusion. Radiol. Med. 114, 461–474.
Scriver, C.R., 2007. The PAH gene, phenylketonuria, and a paradigm shift. Hum. Mutat. 28, 831–845.
Smith, S.M., Johansen-Berg, H., Jenkinson, M., Rueckert, D., Nichols, T.E., Klein, J.C., Robson, M.D., Jones, D.K., Behrens, T.E.J., 2007. Acquisition and voxelwise analysis of multi-subject diffusion data with tract-based spatial statistics. Nat. Protoc. 2, 499–503. https://doi.org/10.1038/nprot.2007.45.
Thompson, A.J., Tillotson, S., Smith, I., Kendall, B., Moore, S.G., Brenton, D.P., 1993. Brain MRI changes in phenylketonuria: associations with dietary status. Brain 116, 811–821.
Van Wegberg, A.M.J., MacDonald, A., Ahring, K., Bélanger-Quintana, A., Blau, N., Bosch, A.M., Burlina, A., Campistol, J., Feillet, F., Giżewska, M., Huijbregts, S.C., Kearney, S., Leuzzi, V., Maillot, F., Muntau, A.C., Van Rijn, M., Trefz, F., Walter, J.H., Van Spronsen, F.J., 2017. The complete European guidelines on phenylketonuria: diagnosis and treatment. Orphanet J. Rare Dis. 12, 1–56. https://doi.org/10.1186/s13023-017-0685-2.
Vermathen, P., Robert-Tissot, L., Pietz, J., Lutz, T., Boesch, C., Kreis, R., 2007. Characterization of white matter alterations in phenylketonuria by magnetic resonance relaxometry and diffusion tensor imaging. Magn. Reson. Med. 58, 1145–1156.
Waisbren, S.E., Noel, K., Fahrbach, K., Cella, C., Frame, D., Dorenbaum, A., Levy, H., 2007. Phenylalanine blood levels and clinical outcomes in phenylketonuria: a systematic literature review and meta-analysis. Mol. Genet. Metab. 92, 63–70. https://doi.org/10.1016/j.ymgme.2007.05.006.
Waters, D., Adeloye, D., Woolham, D., Wastnedge, E., Patel, S., Rudan, I., 2018. Global birth prevalence and mortality from inborn errors of metabolism: a systematic analysis of the evidence. J. Glob. Health 8.
Wechsler, D., 1999. Wechsler Abbreviated Scale of Intelligence (WASI). The Psychological Corporation, San Antonio, TX.
White, D.A., Connor, L.T., Nardos, B., Shimony, J.S., Archer, R., Snyder, A.Z., Moinuddin, A., Grange, D.K., Steiner, R.D., McKinstry, R.C., 2010. Age-related decline in the microstructural integrity of white matter in children with early- and continuously-treated PKU: a DTI study of the corpus callosum. Mol. Genet. Metab. 99, S41–S46 Supple.
White, D.A., Antenor-Dorsey, J.A.V., Grange, D.K., Hershey, T., Rutlin, J., Shimony, J.S., McKinstry, R.C., Christ, S.E., 2013. White matter integrity and executive abilities following treatment with tetrahydrobiopterin (BH4) in individuals with phenylketonuria. Mol. Genet. Metab. 110, 213–217. https://doi.org/10.1016/j.ymgme.2013.07.010.
Wierenga, L., Langen, M., Ambrosino, S., van Dijk, S., Oranje, B., Durston, S., 2014a. Typical development of basal ganglia, hippocampus, amygdala and cerebellum from age 7 to 24. Neuroimage 96, 67–72. https://doi.org/10.1016/j.neuroimage.2014.03.072.
Wierenga, L., Langen, M., Oranje, B., Durston, S., 2014b. Unique developmental trajectories of cortical thickness and surface area. Neuroimage 87, 120–126. https://doi.org/10.1016/j.neuroimage.2013.11.010.
Woltman, H., Feldstain, A., MacKay, C., Rocchi, M., 2012. An introduction to hierarchical linear modeling. Tutor. Quant. Methods Psychol. 8, 52–69. https://doi.org/10.2307/2095731.